

The circular capillary jump

Rajesh K. Bhagat^{1,†} and P. F. Linden¹

¹Department of Applied Mathematics and Theoretical Physics, Wilberforce Road,
Cambridge CB3 0WA, UK

(Received 24 July 2019; revised 31 March 2020; accepted 15 April 2020)

In this paper we re-examine the flow produced by the normal impact of a laminar liquid jet onto an infinite plane when the flow is dominated by surface tension. Over the range of parameters we consider, which are typical of water from a tap over a kitchen sink, it is observed experimentally that after impact the liquid spreads radially over the plane away from the point of impact in a thin film. It is also observed that, at a finite radius, there is an abrupt increase in thickness of the film which has been identified as a hydraulic jump. Once the jump is formed this radius remains constant in time and, further, is independent of the orientation of the surface showing that gravity is unimportant (Bhagat *et al.*, *J. Fluid Mech.*, vol. 851, 2018, R5). We show that the application of conservation of momentum in the film, subject only to viscosity and surface tension and ignoring gravity completely, predicts a singularity in the curvature of the liquid film and consequently a jump in the depth of the film at a finite radius. This location is almost identical to the radius of the jump predicted by conservation of energy and agrees with experimental observations. We also provide the correct boundary condition to be applied at an interface, where there is a change in interfacial area as a result of the fluid flow, that accounts for the energy change associated with fluid molecules' exchange between the interface and the bulk.

Key words: thin films, capillary waves, interfacial flows (free surface)

1. Introduction

In a recent paper Bhagat *et al.* (2018) conducted experiments that showed that in a thin liquid film, on scales typical of those found in a kitchen sink, the circular jump produced by the normal impact of a round laminar jet onto an infinite plane is independent of the orientation of the surface. These experiments conclusively showed that gravity does not play a significant role in the origin/formation of these jumps – in sharp contrast with previous theoretical analyses. They also used conservation of energy, including both surface tension and gravity, to determine the radius of the jump. As we discuss below, on the scale of a kitchen sink the predicted radius is found to be almost independent of gravity, and is in excellent agreement with experiments, which cover fluids with a range of surface tension values.

[†] Email address for correspondence: rkb29@cam.ac.uk

Since the conclusions of Bhagat *et al.* (2018) are markedly different from the accepted view of the role of gravity in these thin-film jumps the paper has attracted criticism, most particularly in a recent paper by Duchesne, Andersen & Bohr (2019) who, despite the experimental evidence, continue to question the role of surface tension in these flows. The underlying issue appears to be the current understanding of the interfacial flow which is that, in both in hydrostatics and in hydrodynamics, the influence of surface tension (when surface tension is uniform) is fully expressed as a pressure, commonly known as the Laplace pressure. The argument is that the force due to surface tension, which acts a tensile force at the line boundary of the interfacial surface, is mathematically equivalent to a pressure normal to the interface and, since the liquid velocity is tangential to the interface, this force can do no work. For hydrostatics, we have no argument with this viewpoint, but in hydrodynamics, we will show that the interfacial surface energy is not conserved, except when the liquid film is completely flat and surface tension force is trivially balanced.

Before proceeding further with this discussion we note that the importance of surface tension had previously been noted by Mohajer & Li (2015) who measured the jump radius and the height of the liquid downstream of the jump for water and a water–surfactant solution (see their figures 4 and 13). They observed a significant increase in the jump radius when the surface tension was reduced by the addition of the surfactant. They also reported that for a range of flow rates the jump height remained constant and depended only on the surface tension of the liquid.

Despite this experimental evidence several other recent papers (Fernandez-Feria, Sanmiguel-Rojas & Benilov 2019; Scheichl 2019; Sen *et al.* 2019; Wang & Khayat 2019) continue to support the previous gravity-based theory. For example, Fernandez-Feria *et al.* (2019) performed numerical simulations of the downward vertical impingement of a liquid jet onto a horizontal plate and compared their results with the experimental data from Button *et al.* (2010), which were obtained for an upward directed jet onto a ceiling. Despite the opposite vertical orientations the authors concluded gravity is the dominant force.

The role of surface tension is subtle, and one objective of this paper is to clarify the contribution of surface tension to the dynamics. The other objective is to show that the jump radius can be predicted using momentum conservation and show that this is consistent with the energy-based approach used by Bhagat *et al.* (2018). In order to focus on the role of surface tension we predict the jump location using conservation of momentum, ignoring gravity completely.

Conventionally, the circular jump has been studied in an experimental arrangement where a vertical jet impinges onto a horizontal plate and either flows over a weir or off the edge of the plate. In this paper we are concerned with the situation in which the plate is effectively an infinite plane and we consider the jump before the spreading liquid film encounters either the weir or the edge. The observations of Bhagat *et al.* (2018) show (for sufficiently high Reynolds numbers) that the jump, once formed, has a constant radius until the spreading film reaches the edge of the plate. In practice, once the film reaches the edge of the plate a different boundary condition is imposed that changes the depth of the downstream subcritical film, which, in turn, changes the position of the previously formed jump. Usually, in this later adjustment, since the subcritical region is significantly deeper than the supercritical region upstream of the jump, gravity can play a significant role. However, we will show that until the further downstream condition influences the jump, the initial jump location is determined by surface tension alone.

The paper is organised as follows. We begin in § 2 by a consideration of dimensional analysis which will set the parameter ranges that are appropriate for our

theoretical analysis. The role of surface tension at the liquid–gas interface in a flowing, as distinct from stationary, liquid is derived and applied to a radially spreading thin film in §3. A prediction for the jump radius is then obtained from application of conservation of momentum in both the radial and film-normal directions in §4. The energy-based approach presented in Bhagat *et al.* (2018) is revisited and compared with the momentum based approach in §5. In §6, we discuss the relative importance of surface tension and re-visit the analysis of Duchesne *et al.* (2019) and discuss the flaw in their theory. Finally, our conclusions are given in §7.

2. Dimensional analysis

We begin by considering the implications of dimensional analysis. The relative importance of gravity g and surface tension depends on the fluid properties, the value of the surface tension γ , the density ρ and kinematic viscosity ν and the flow characterised by the jet flow rate Q . Dimensional analysis shows that when either gravity or surface tension is ignored the jump radius scales, respectively, as

$$R_{ST} \sim \frac{Q^{3/4} \rho^{1/4}}{\nu^{1/4} \gamma^{1/4}} \quad \text{or} \quad R_G \sim \frac{Q^{5/8}}{\nu^{3/8} g^{1/8}}. \quad (2.1a,b)$$

In a particular flow the jump will either be caused by surface tension if $R_{ST} < R_G$ and gravity if $R_{ST} > R_G$. This criterion leads to a critical flow rate Q_C given by

$$Q_C = \frac{\gamma^2}{\nu \rho^2 g}, \quad (2.2)$$

below which surface tension is the dominant force and above which gravity is important. For water $Q_C \approx 500 \text{ cm}^3 \text{ s}^{-1}$ (i.e. $\approx 30 \text{ l min}^{-1}$), which is significantly larger than the flow in the standard kitchen sink.

In appendix A (see (A 2)) we further show that including gravity provides a correction to the radius predicted by surface tension. This correction to the pure surface tension radius R_{ST} takes the values 0.95 and 0.77, for $Q = 2Q_C$ and $10Q_C$, respectively, which shows that even for $Q \sim 10Q_C$, the jump is dominated by the surface tension of the liquid. Table 1 gives values of Q_C for liquids used in experiments (Bohr, Dimon & Putkaradze 1993; Bhagat *et al.* 2018; Duchesne *et al.* 2019) and we see that $Q \ll Q_C$ in the experiments in water, and that the flow rates are only close to Q_C in the experiments with ethylene glycol and silicone oil. However, as we note from (A 2), even in these latter cases this scaling analysis implies that surface tension is still dominant. Consequently, we conclude that all the experiments listed in table 1 are expected to fall within the range of parameters to which the theory developed below that ignores gravity is expected to apply.

It is also worth noting that apart from surface tension the only parameters that have been varied in experiments are the viscosity and jet flow rate. The scaling relations (2.1) have very similar dependences on these two parameters, which makes it very hard to distinguish between them on experimental grounds alone. This is possibly why some controversy persists about the interpretation of the experimental observations.

3. Theory

3.1. Surface forces and energy in hydrodynamics

Surface forces at a liquid interface arise from short range intermolecular interactions and the total short range force acting on a fluid element is determined by the surface area of the element, while the volume of the element is not relevant for such forces (Batchelor 2000). The molecular origin of surface tension and surface energy is

Liquid	Reference	Q (cm ³ s ⁻¹)	Q_c (cm ³ s ⁻¹)	$\gamma \times 10^{-3}$ (kg s ⁻²)	$\nu \times 10^{-6}$ (m s ⁻²)	ρ (kg m ⁻³)
Water	Mohajer & Li (2015)	2.5–8.33	518	72	1.002	1000
Ethylene glycol	Rojas <i>et al.</i> (2010)	20	22	45	7.6	1100
Silicon oil – 1	Duchesne, Lebon & Limat (2014)	4.3–60	2.3	20	20	950–965
Silicon oil – 2	Duchesne <i>et al.</i> (2014)	—	0.45	20	98	950–965
WP95/5	Bhagat <i>et al.</i> (2018)	83–200	82	42.5	1.274	989
WP80/20	Bhagat <i>et al.</i> (2018)	83–200	58	26	2.30	968
SDBS	Bhagat <i>et al.</i> (2018)	83–200	147	38	1	1000

TABLE 1. Parameters used in published experiments. The jet flow rate Q , the critical flow rate Q_c at which gravity begins to play a role, the surface tension γ , the kinematic viscosity ν and the density ρ of the fluid.

associated with intermolecular cohesive forces. The average free energy associated with a fluid molecule in the liquid bulk, where it is surrounded by similar molecules is independent of its position. However, within a distance less than the range of the cohesive forces (10^{-9} m) from the interface, the liquid molecules have an additional free energy which is proportional to the interfacial surface area. A net exchange of liquid molecules between the interface and the bulk that necessarily accompanies a change in surface area will be associated with a net energy exchange.

Now consider the case of an impacting liquid jet and follow the small material volume of fluid, $\pi a^2 l$ in the jet (indicated as 0 in figure 1), where a is the radius of the jet and l is the length of the cylindrical fluid element. The surface area of a liquid interface changes as it spreads on the plane as a thin film of thickness h , and it is straightforward to show that the ratio of the final to initial surface area is $a/2h$. In the spreading film when h decreases with radius and $a/2h \gg 1$, implying that there is an energy penalty as liquid molecules leave the bulk to increase the surface area of the spreading film. Whereas, at the hydraulic jump, an abrupt increase of liquid film thickness implies a release of the surface energy. This clearly demonstrates that even in a steady flow a spatial variation of liquid film thickness implies an active exchange of mechanical and surface energy. We now discuss the way in which this exchange of energy is accounted for.

3.2. Surface tension and the interfacial boundary condition

Fluid motion is governed by the Navier–Stokes equations which express conservation of momentum in a fluid continuum. For flows with an interface between two fluids, the Navier–Stokes equations do not express the surface tension force acting on the interface. This force is introduced as a normal stress boundary condition at the interface.

Consider a fixed surface S , with unit normal \mathbf{n} , bounded by a closed contour C with the line element $d\mathbf{l}$ around the contour in the interface between two immiscible fluids, taken here for simplicity to be the common case of a liquid and a gas denoted by the subscripts L and G , respectively, with constant surface tension γ (see figure 2). Since the surface tension force acts in a direction perpendicular to \mathbf{n} and the contour C , continuity of the normal stress is expressed as

$$\int_S (\mathbf{T}_G - \mathbf{T}_L) \cdot \mathbf{n} dS + \gamma \int_C d\mathbf{l} \times \mathbf{n} = 0, \quad (3.1)$$

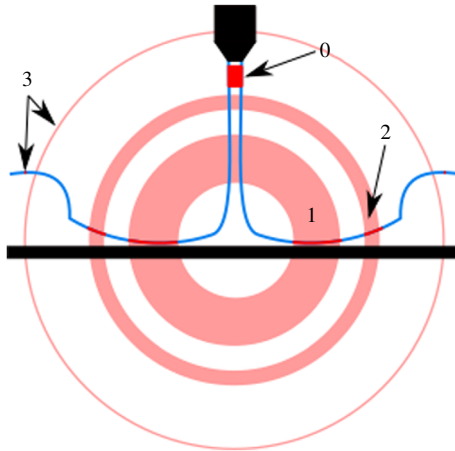


FIGURE 1. An illustrative sketch of a circular hydraulic jump on an infinite plate that was reported experimentally by Bhagat *et al.* (2018), along with a history of the interfacial surface area of a material fluid volume, $V = \pi a^2 l$ (indicated as 0), where a is the radius of the jet. The annular surfaces are the top views of the surface of the material volume at different instances when it passes through locations 1 and 2 in the supercritical region and 3 in subcritical region. The surface area of the material volume is inversely proportional to the liquid film thickness h , which in the supercritical region where h decreases implies an increase in surface area. At the location of hydraulic jump an abrupt change of liquid film thickness implies a release of the surface energy.

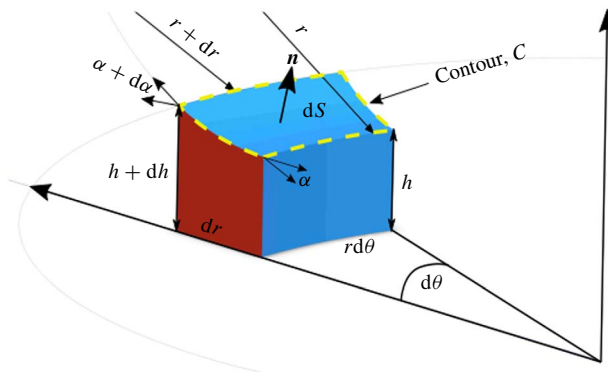


FIGURE 2. A schematic of the differential control volume showing the slope of the thin liquid film, and a contour, C enclosing an interfacial surface, S .

where $\mathbf{T} = -p\mathbf{I} + \mu[\nabla\mathbf{u} + (\nabla\mathbf{u})^T]$ is the total stress, with pressure p and velocity \mathbf{u} , and μ is the dynamic viscosity of the fluid. Using the vector identity and $\int_C d\mathbf{l} \times \mathbf{n} \equiv -\int_S (\nabla_s \cdot \mathbf{n})\mathbf{n} dS$,

$$\int_S (\mathbf{T}_G - \mathbf{T}_L) \cdot \mathbf{n} dS = \gamma \int_S (\nabla_s \cdot \mathbf{n})\mathbf{n} dS. \tag{3.2}$$

Since the surface S is arbitrary, we then obtain the conventional form of the dynamic boundary condition

$$(\mathbf{T}_G - \mathbf{T}_L) \cdot \mathbf{n} = \gamma(\nabla_s \cdot \mathbf{n})\mathbf{n}, \tag{3.3}$$

where $\nabla_s = [\mathbf{I} - \mathbf{nn}] \cdot \nabla$ is the surface gradient, relating the jump in the normal stress to the curvature of the surface in agreement with Bush & Aristoff (2003) and valid pointwise in space. However, it is important to note that the surface tension forces act along the local tangents at different points of the closed contour C , and it is the net resultant of these tensile forces that acts along the normal to the interface. In the case of a stationary liquid and gas, the viscous term is zero, and this equation gives the usual Laplace pressure in the liquid associated with the curvature of the surface. In the case of a flowing liquid, (3.3) will give the correct net resultant force on an interfacial surface S , but does not give a detailed account of the tensile forces along the contour C . The velocity of the liquid may vary around the contour C implying that liquid molecules crossing the boundary may not be conserved and need to be accounted for in the surface energy exchange. We consider this effect in the next section.

3.3. Interfacial surface energy conservation

Assuming the dynamic viscosity of the gas (for air and water the ratio $\mu_a/\mu_w \sim 10^{-2}$) is negligible compared to that of the liquid and that the velocities in the liquid and gas are comparable, and denoting pressure in the gas as p_G and in the liquid as p_L , (3.1) can be written as

$$\int_S (-p_G + p_L)\mathbf{n} \, dS - \mu \int_S \mathbf{n} \cdot [\nabla \mathbf{u} + (\nabla \mathbf{u})^T] \, dS + \gamma \int_C d\mathbf{l} \times \mathbf{n} = 0, \tag{3.4}$$

where \mathbf{u} is the velocity in the liquid at the interface. The surface energy flux can be calculated by taking a dot product between the interfacial velocity at the contour C and the forces to obtain (since $\mathbf{u} \cdot \mathbf{n} = 0$ on the interface)

$$\mu \int_S \mathbf{u} \cdot (\mathbf{n} \cdot [\nabla \mathbf{u} + (\nabla \mathbf{u})^T]) \, dS = \gamma \int_C \mathbf{u} \cdot (d\mathbf{l} \times \mathbf{n}), \tag{3.5}$$

which can be re-expressed as

$$\begin{aligned} \mu \int_S \{\mathbf{u} \cdot [(\mathbf{n} \cdot \nabla)\mathbf{u}] + \mathbf{n} \cdot [(\mathbf{u} \cdot \nabla)\mathbf{u}]\} \, dS &= \gamma \int_S \{(\nabla_I \cdot \mathbf{u}) - [(\mathbf{n} \cdot \nabla_I)\mathbf{u}] \cdot \mathbf{n}\} \, dS, \\ &= \gamma \frac{DS}{Dt}, \end{aligned} \tag{3.6}$$

the rate of change of the material surface area S (see (3.1.5) of Batchelor (2000)), where the subscript I of the operator ∇_I is to emphasise that the operator is applied at the interface only.

Thus the increase in surface energy is supplied by the kinetic energy of the flow, which, of course, is zero in the case of stationary liquid. We also emphasise that the velocity field here is the surface velocity field, for which $(\nabla_I \cdot \mathbf{u})$ may or may not be equal to zero due to the addition (or loss) of fluid elements to the liquid interface as discussed above. The surface energy will only be conserved when the velocity field at the interface satisfies the condition $\{(\nabla_I \cdot \mathbf{u}) - [(\mathbf{n} \cdot \nabla_I)\mathbf{u}] \cdot \mathbf{n}\} = 0$ (which is satisfied for a flat surface for which net force due to surface tension is zero), otherwise there will be an active energy exchange with the bulk.

It is important to re-emphasise that the pointwise dynamic boundary condition in its conventional form (3.3), which if used to calculate the surface energy over a surface S does not account for the variation in velocity along the contour C , will give a flawed result implying that the net surface energy exchange is zero. We emphasise that (3.6) is the correct interfacial boundary condition to be applied at the liquid interface and will be used in the analysis below.

4. Momentum conservation

We now apply conservation of momentum to the axisymmetric flow spreading radially from the point of impact of the jet on the plane, ignoring gravity. In cylindrical coordinates (r, θ) with the origin at the point of jet impact, let u, w be the radial and vertical velocity components, respectively.

First we determine the surface boundary condition. Following Bush & Aristoff (2003), we write the equation of the axisymmetric surface in implicit form

$$J(r, z) = z - h(r) = 0, \tag{4.1}$$

which yields the vector normal to the film surface

$$\mathbf{n} = \frac{\nabla J}{|\nabla J|} = \frac{\hat{\mathbf{z}} - h'\hat{\mathbf{r}}}{(1 + h'^2)^{1/2}}, \tag{4.2}$$

where $\hat{\mathbf{r}}$ and $\hat{\mathbf{z}}$ are unit vectors in the radial and wall-normal directions, respectively, and $h' = dh/dr$. We define the angle α as the tangent to the surface defined by $h' = \tan \alpha$. Then $\cos \alpha = 1/(1 + h'^2)^{1/2}$ and $\sin \alpha = h'/(1 + h'^2)^{1/2}$, and (4.2) can also be written as

$$\mathbf{n} = \hat{\mathbf{z}} \cos \alpha - \hat{\mathbf{r}} \sin \alpha. \tag{4.3}$$

We denote the radial velocity component at the surface $z = h$ as $u_s(r)$. From the kinematic boundary condition the vector surface velocity can be written as

$$\mathbf{u} = u_s(r)\hat{\mathbf{r}} + u_s(r)h'(r)\hat{\mathbf{z}}, \tag{4.4}$$

which implies that, at the interface,

$$\{(\nabla_I \cdot \mathbf{u}) - [(\mathbf{n} \cdot \nabla_I)\mathbf{u}] \cdot \mathbf{n}\} = \frac{1}{r} \frac{d(u_s r)}{dr} + \frac{u_s h' h''}{(1 + h'^2)} = \frac{1}{r(1 + h'^2)^{(1/2)}} \frac{d\{u_s r(1 + h'^2)^{(1/2)}\}}{dr}. \tag{4.5}$$

Substituting (4.5) in (3.6) and recognising $dS = r(1 + h'^2)^{(1/2)} d\theta dr$ yields

$$\mu \int_S \{\mathbf{u} \cdot [(\mathbf{n} \cdot \nabla)\mathbf{u}] + \mathbf{n} \cdot [(\mathbf{u} \cdot \nabla)\mathbf{u}]\} dS = \gamma \int_S \frac{d\{u_s r(1 + h'^2)^{(1/2)}\}}{dr} dr d\theta. \tag{4.6}$$

Note that these results depend only on the surface velocity and hold independent of the wall-normal velocity profile. However, in order to obtain an explicit momentum equation, we need to calculate the shape factors arising due to the velocity profile. We recognise that a similarity velocity profile in wall-normal direction will not satisfy the zero interfacial stress condition $(\mathbf{n} \cdot \nabla)\mathbf{u} \neq 0$ (see appendix B). Nevertheless, the liquid film upstream of the hydraulic jump remains almost flat, and the shape factor is not

expected to change much in the radial direction. Therefore, we use the Watson (1964) velocity in similarity form to calculate the shape factor

$$u(r, z) = u_s(r)f(\eta), \quad \eta \equiv \frac{z}{h(r)}, \quad 0 \leq \eta \leq 1, \tag{4.7a,b}$$

where u_s as above is the surface velocity and $f(0) = 0, f(1) = 1$. Conservation of mass implies

$$\int_0^h ur \, dz = ru_s h \int_0^1 f(\eta) \, d\eta \equiv C_1 u_s r h = Q/2\pi, \tag{4.8}$$

and $C_1 \equiv \int_0^1 f(\eta) \, d\eta$ is an integration constant arising from the velocity profile. Incompressibility gives

$$w = - \int_0^\eta \frac{1}{r} \frac{\partial ru}{\partial r} \, dz = - \frac{1}{r} \frac{d}{dr} \left[(ru_s h) \int_0^\eta f(\eta) \, d\eta \right].$$

Then, using (4.8),

$$w = -u_s h \frac{d}{dr} \int_0^\eta f(\eta) \, d\eta = uh' \eta = u_s h' \eta f(\eta), \tag{4.9}$$

which automatically satisfies the kinematic boundary conditions at the wall and interface. We now use these expressions for the velocity in equations expressing momentum conservation in the radial and wall-normal directions.

4.1. Force on an axisymmetric thin film

For the control volume shown in figure 2, with the interface bounded by the closed contour C , the differential arc length $d\mathbf{l} = (r \, d\theta) \hat{\boldsymbol{\theta}}|_r^{r+dr} - (dr) \hat{\mathbf{r}}|_\theta^{\theta+d\theta} - (dh) \hat{\mathbf{z}}|_\theta^{\theta+d\theta}$. Consequently, the force due to surface tension on this interface is

$$dF_\gamma = \gamma(d\mathbf{l} \times \mathbf{n}) = \gamma(d\theta r \cos \alpha \hat{\mathbf{r}})|_r^{r+dr} + \gamma(d\theta r \sin \alpha \hat{\mathbf{z}})|_r^{r+dr} + \gamma \left(\frac{dr}{\cos \alpha} \hat{\boldsymbol{\theta}} \right) \Big|_\theta^{\theta+d\theta}. \tag{4.10}$$

Considering the circular symmetry, in the limit of dr and $d\theta \rightarrow 0$

$$dF_\gamma = \left(\gamma d(r \cos \alpha) - \gamma \frac{dr}{\cos \alpha} \right) d\theta \hat{\mathbf{r}} + \gamma d(r \sin \alpha) d\theta \hat{\mathbf{z}}. \tag{4.11}$$

Therefore, from (3.5) and (4.11), the radial and vertical components of the normal stress at the free surface can be written as

$$\begin{aligned} F_{\gamma,r} &\equiv \int_r^{r+dr} \mu(\mathbf{n} \cdot [\nabla \mathbf{u} + (\nabla \mathbf{u})^T]) \cdot \hat{\mathbf{r}} \left(r \, d\theta \frac{dr}{\cos \alpha} \right) \Big|_h = \int_r^{r+dr} P \sin \alpha r \, d\theta \frac{dr}{\cos \alpha} \\ &+ \gamma r \, d\theta \cos \alpha|_r^{r+dr} - \gamma \frac{dr}{\cos \alpha} \, d\theta, \end{aligned} \tag{4.12}$$

and

$$\begin{aligned} F_{\gamma,z} &\equiv \int_r^{r+dr} \mu(\mathbf{n} \cdot [\nabla \mathbf{u} + (\nabla \mathbf{u})^T]) \cdot \hat{\mathbf{z}} \left(r \, d\theta \frac{dr}{\cos \alpha} \right) \Big|_h \\ &= \int_r^{r+dr} P r \, d\theta \, dr + r \, d\theta \gamma \sin \alpha \Big|_r^{r+dr}, \end{aligned} \tag{4.13}$$

where $P = p_L - p_G$. As we will see below, application of momentum conservation requires expressions for the radial gradients of these forces, and as axisymmetry implies we can drop $d\theta$, these are given by

$$\begin{aligned} \frac{dF_{\gamma,r}}{dr} &= \frac{d}{dr} \left(\int_r^{r+dr} \mu(\mathbf{n} \cdot [\nabla\mathbf{u} + (\nabla\mathbf{u})^T]) \cdot \hat{\mathbf{r}} \left(\frac{r \, dr}{\cos \alpha} \right) \Big|_h \right) \\ &= rP \tan \alpha - \frac{\gamma}{\cos \alpha} + \gamma \frac{d(r \cos \alpha)}{dr} \end{aligned} \tag{4.14}$$

and

$$\frac{dF_{\gamma,z}}{dr} = \frac{d}{dr} \left(\int_r^{r+dr} \mu(\mathbf{n} \cdot [\nabla\mathbf{u} + (\nabla\mathbf{u})^T]) \cdot \hat{\mathbf{z}} \left(\frac{r \, dr}{\cos \alpha} \right) \Big|_h \right) = rP + \gamma \frac{d(r \sin \alpha)}{dr}. \tag{4.15}$$

4.2. Momentum balance in the radial direction

In the absence of gravity, the momentum equation in the radial direction is

$$\rho \left(u \frac{\partial u}{\partial r} + w \frac{\partial u}{\partial z} \right) = \frac{1}{r} \frac{\partial(r\tau_{rr})}{\partial r} + \frac{\partial\tau_{rz}}{\partial z}, \tag{4.16}$$

where $\tau = T + p\mathbf{I}$ is the total stress consisting of the deviator stress T and the pressure p (in cylindrical coordinates). Since the pressure in the gas at the surface is constant (atmospheric) and the film is thin, the radial pressure gradient in the liquid is only a function of radius caused by the curvature of the surface.

We use incompressibility ($\nabla \cdot \mathbf{u} = 0$ in the bulk fluid), integrate (4.16) across the film from the wall to the interface, use axisymmetry to eliminate $d\theta$, substitute for the velocity from (4.7) and (4.9) and apply the surface tension boundary condition (4.5), to obtain

$$\frac{d}{dr} \int_0^h \rho r u^2 \, dz = - \int_0^h \frac{dp}{dr} r \, dz + rP \tan \alpha - \frac{\gamma}{\cos \alpha} + \gamma \frac{d(r \cos \alpha)}{dr} - \mu r \left(\frac{\partial u}{\partial z} + \frac{\partial w}{\partial r} \right) \Big|_0. \tag{4.17}$$

Noting that conservation of mass (4.8) implies $u_s r h = \text{const.}$, we obtain

$$C_2 \left[\rho u_s r h \frac{du_s}{dr} \right] = - \frac{dp}{dr} r h + rP \tan \alpha - \frac{\gamma}{\cos \alpha} + \gamma \frac{d(r \cos \alpha)}{dr} - \mu r \left(\frac{\partial u}{\partial z} + \frac{\partial w}{\partial r} \right) \Big|_0, \tag{4.18}$$

where $C_2 = \int_0^1 f^2(\eta) \, d\eta$ is a second integration constant. Equation (4.18) can be written in terms of the interface slope

$$\begin{aligned} C_2 \left[\rho u_s r h \frac{du_s}{dr} \right] &= - \frac{dp}{dr} r h + r p h' - \gamma(1 + h^2)^{1/2} + \gamma \frac{1}{(1 + h^2)^{1/2}} \\ &\quad - \gamma \frac{r h' h''}{(1 + h^2)^{3/2}} - \tau_w r, \end{aligned} \tag{4.19}$$

where $\tau_w = -\mu(\partial u/\partial z + \partial w/\partial r)|_0$ is the wall shear stress.

4.3. Momentum balance in the wall-normal direction

We now apply conservation of momentum in the wall-normal z direction in the differential control volume shown in figure 2. Since the film is thin, the pressure is independent of z and for an axisymmetric flow

$$\rho u r \frac{\partial w}{\partial r} + \rho w r \frac{\partial w}{\partial z} = \frac{\partial(r\tau_{rz})}{\partial r} + r \frac{\partial \tau_{zz}}{\partial z}. \tag{4.20}$$

As before, we integrate across the film to obtain

$$\int_0^h \rho u r \frac{\partial w}{\partial r} dz + \int_0^h \rho w r \frac{\partial w}{\partial z} dz = \int_0^h \frac{\partial(r\tau_{rz})}{\partial r} dz - 2\mu r \left. \frac{\partial w}{\partial z} \right|_h. \tag{4.21}$$

Substituting for the velocity from (4.7) and (4.9) gives

$$\begin{aligned} & \rho u_s r h \frac{d(u_s h')}{dr} \int_0^1 \eta f^2(\eta) d\eta - \rho h^2 u_s^2 r \int_0^1 \eta f^2(\eta) d\eta - \rho \left. \frac{u_s^2 r h^2 \eta^2 f^2(\eta)}{2} \right|_0^1 \\ & + \rho h^2 u_s^2 r \int_0^1 \eta f^2(\eta) d\eta + r \left. \frac{\rho w^2}{2} \right|_0^h = \frac{dF_{\gamma,z}}{dr} - \int \frac{\partial(r\tau_{rz})}{\partial r} dz \Big|_0^h - 2\mu r \left. \frac{\partial w}{\partial z} \right|_h. \end{aligned} \tag{4.22}$$

Substituting (4.15) into (4.22) yields

$$\begin{aligned} & \rho u_s r h \frac{d(u_s h')}{dr} \int_0^1 \eta f^2(\eta) d\eta \\ & = rP + \gamma \frac{d(r \sin \alpha)}{dr} - \int \frac{\partial(r\tau_{rz})}{\partial r} dz \Big|_0^h - 2\mu r \left. \frac{\partial w}{\partial z} \right|_h, \\ & = rP + \gamma \sin \alpha + \gamma r \cos \alpha \frac{d\alpha}{dr} - \int \frac{\partial(r\tau_{rz})}{\partial r} dz \Big|_0^h - 2\mu r \left. \frac{\partial w}{\partial z} \right|_h, \\ & = rP + \frac{\gamma h'}{(1+h^2)^{1/2}} + \frac{\gamma r h''}{(1+h^{3/2})} - \int \frac{\partial(r\tau_{rz})}{\partial r} dz \Big|_0^h - 2\mu r \left. \frac{\partial w}{\partial z} \right|_h. \end{aligned} \tag{4.23}$$

In the thin liquid film upstream of the hydraulic jump, the interface slope remains small and we will ignore the higher-order terms in dh/dr . Applying this approximation and re-arranging (4.23) gives an expression for the curvature of the film

$$\begin{aligned} & h'' (\rho u_s^2 r h \int_0^1 \eta f^2(\eta) d\eta - \gamma r) + h' \left(\rho u_s r h \frac{du_s}{dr} \int_0^1 \eta f^2(\eta) d\eta - \gamma \right) \\ & = rP - \int \frac{\partial(r\tau_{rz})}{\partial r} dz \Big|_0^h - 2\mu r \left. \frac{\partial w}{\partial z} \right|_h. \end{aligned} \tag{4.24}$$

Finally, substituting $\rho u_s r h (du_s/dr)$ from the radial momentum balance (4.19) gives

$$\begin{aligned} & [C_3 \rho u_s^2 r h - \gamma r] h'' + \frac{C_3}{C_2} h' \left(-\frac{dP}{dr} r h + r P h' - \gamma (1+h^2)^{1/2} + \gamma \frac{1}{(1+h^2)^{1/2}} \right. \\ & \left. - \gamma \frac{h' h''}{(1+h^2)^{3/2}} - \tau_w r - \frac{C_2}{C_3} \gamma \right) = rP - \int \frac{\partial(r\tau_{rz})}{\partial r} dz \Big|_0^h - 2\mu r \left. \frac{\partial w}{\partial z} \right|_h, \end{aligned} \tag{4.25}$$

where $C_3 = \int_0^1 \eta f^2(\eta) d\eta$ is a third integration constant.

Ignoring higher-order terms in h' and re-arranging gives an expression for the curvature of the film

$$h'' = \frac{-h' \frac{C_3}{C_2} \left[-\frac{dP}{dr} rh + r\tau_w - \frac{C_2}{C_3} \gamma \right] + rP + \int \frac{\partial(r\tau_{rz})}{\partial r} dz \Big|_0 - 2\mu r \frac{\partial w}{\partial z} \Big|_h}{C_3 \rho u_s^2 rh(1 - We^{-1})}, \tag{4.26}$$

where the Weber number We is defined by

$$We \equiv \frac{C_3 \rho u_s^2 h}{\gamma}. \tag{4.27}$$

Consequently, we predict a singularity in the curvature of the film at a critical radius where the film thickness is such that $We = 1$. This criterion gives the location of the hydraulic jump.

4.4. Revisiting the radial momentum balance

We now revisit the radial momentum balance (4.19), which can also be written as

$$C_2[\rho u_s rh du_s] = -rh dp + rp dh - \gamma(1 + h^2)^{1/2} dr + \gamma \frac{dr}{(1 + h^2)^{1/2}} - \gamma \frac{rh'h'' dr}{(1 + h^2)^{3/2}} - \tau_w r dr, \tag{4.28}$$

and apply it at the jump radius. We note that the jump is a singularity (see figure 3b), where $dh/dr = \tan \alpha \rightarrow \infty$, $dr \rightarrow 0$, $dh = H$, a finite quantity, and α changes from 0 to $\pi/2$, and the radial velocity changes from u_s to 0. Substituting the trigonometric forms of the functions and integrating (4.28) at the jump location $r = R$ gives

$$\int C_2 \rho u_s R h du_s = - \int R h dp + \int R p dh - \int \gamma \sin \alpha dh + \gamma R \cos \alpha \Big|_0^{\pi/2} + \int \gamma \cos \alpha dr - \int \tau_w R dr. \tag{4.29}$$

Then in scaled terms (4.29) can be written

$$-C_2 \rho u_s^2 R h \approx RH \left(p - \frac{\gamma}{R} \right) - \gamma R. \tag{4.30}$$

Since, at the jump, the pressure p scales as γ/R (see Bush & Aristoff 2003), the first term on the right-hand side of (4.29) is zero, which gives $We = 1$ as the condition for the hydraulic jump. Thus conservation of radial momentum gives a similar result for the jump condition.

5. Relation to energy conservation

For a better physical understanding we can also get the interfacial energy from a consideration of the interfacial force. From (4.11), the energy flux associated with surface tension force on the control volume (figure 2) is

$$dF_\gamma \cdot (u\hat{r} + w\hat{z}) = \gamma(d\theta ur \cos \alpha)|_r^{r+dr} + \gamma(d\theta wr \sin \alpha)|_r^{r+dr}. \tag{5.1}$$

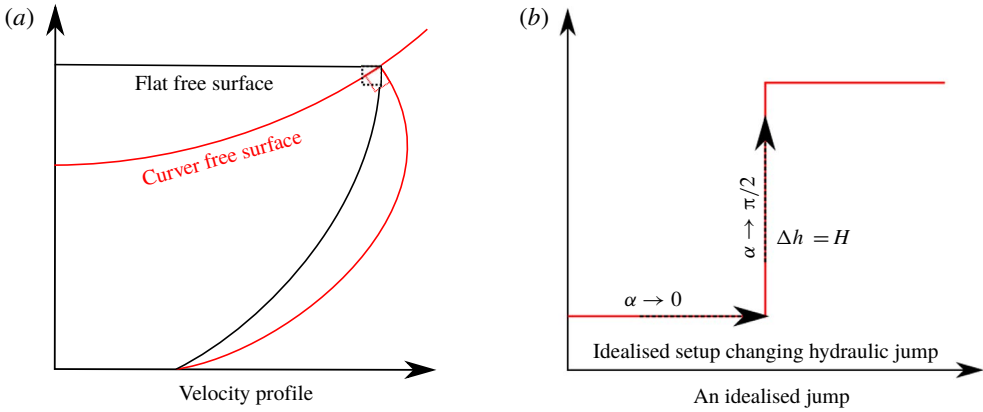


FIGURE 3. (a) Schematic velocity profiles in a flow with conventional flat surface assumption with zero radial viscous stress (black) and liquid interface with zero tangential stress but non-zero radial stress (red). The surface tension force retards the flow in the radial direction and accelerates it in the wall-normal direction, giving non-zero radial and wall-normal viscous stresses at the surface (3.1). (b) An idealised hydraulic jump.

Circular symmetry implies that there is no net flux of fluid in the azimuthal direction and so substituting (4.4) into (5.1) yields

$$dF_\gamma \cdot (u\hat{r} + w\hat{z}) = \gamma(d\theta u_s r(1 + h^2)^{1/2})|_r^{r+dr}, \tag{5.2}$$

which is the equivalent result to (4.6) derived by considering the rate of change of interfacial surface area and work done by the surface tension force. Consequently, in a control volume approach, the force due to surface tension, which appears through the normal stress boundary condition, can be incorporated as a surface force on the circumference of the control volume consistent with the analysis in Bhagat *et al.* (2018).

6. Relative importance of surface tension

We now return to the question of the relative importance of gravity and surface tension in these flows. Duchesne *et al.* (2019) argued that the analysis of Bhagat *et al.* (2018) is wrong and that surface tension does not play a significant role in the formation of these thin-film jumps. Duchesne *et al.* (2019) wrote the energy equation over a volume V bounded by a closed surface A (their equation (13)) as

$$-\int_A [v_j (\frac{1}{2}\rho v_i v_i + p) - \mu v_i v_{i,j}] n_j dA - \frac{1}{2}\mu \int_V v_{i,j}^2 dV = 0, \tag{6.1}$$

where the pressure p is taken to be sum of a Laplace term and a hydrostatic pressure term. Duchesne *et al.* (2019) initially ignore all the viscous terms in (6.1) and integrated the first term over a cylindrical surface spanning the film to obtain (in our notation)

$$\chi(r) = \int_0^h u (\frac{1}{2}\rho(u^2 + w^2) + p) r dz \approx \frac{1}{2}C_3 \rho r u_s^3 h + C_1 u_s r h p. \tag{6.2}$$

They then differentiate this expression with respect to r , and set the derivative χ' equal to the viscous terms which they denote as ξ . This leads to their equation (20), where the viscous terms remain unspecified as ξ . However, the surface energy term $\int \mu v_i v_{i,j} n_j dS$ evaluated at the free surface S is, from (3.6),

$$\int_S \mu v_i v_{i,j} n_j dS \equiv \mu \int_S \{ \mathbf{u} \cdot [(\mathbf{n} \cdot \nabla) \mathbf{u}] + \mathbf{n} \cdot [(\mathbf{u} \cdot \nabla) \mathbf{u}] \} dS = \gamma \int_S \{ (\nabla_I \cdot \mathbf{u}) - [(\mathbf{n} \cdot \nabla_I) \mathbf{u}] \cdot \mathbf{n} \} dS, \tag{6.3}$$

and includes the effect of surface tension and depends on the surface velocity. In their analysis, Duchesne *et al.* (2019) did not include the surface energy term.

Duchesne *et al.* (2019) integrated (6.1) over the inner cylinder of the control volume. Instead, in our analysis we integrate (6.1) for the complete closed annular control volume from 0 to 2π , which yields

$$-\frac{1}{2} C_3 \rho r u_s^3 h|_r^{r+dr} - C_1 u_s r h p|_r^{r+dr} + \gamma d\{u_s r(1 + h'^2)^{(1/2)}\} - \tau_w r dr = 0. \tag{6.4}$$

Recognising that $u_s r h = \text{constant}$, τ_w is the wall friction and dividing (6.4) by dr , the limit of $h' \rightarrow 0$ gives

$$-C_3 \rho r u_s^2 h \frac{du_s}{dr} + \gamma r \frac{du_s}{dr} + \gamma u_s - C_1 u_s r h \frac{dp}{dr} + \tau_w r dr = 0. \tag{6.5}$$

This equation is equivalent to (in the absence of gravity) (5.4) in Bhagat *et al.* (2018) which was obtained from a control volume approach and leads to a critical Weber number of order one at the jump (and not $O(\alpha)$ as Duchesne *et al.* (2019) claim).

Including this surface term (6.3) explicitly in ξ , since it involves u_s and γ , will change the result in Duchesne *et al.* (2019) and leads to the conclusion that surface tension is the dominant force, consistent with the increase in surface area documented in § 3.3.

7. Conclusions

Applying conservation of radial and wall-normal momentum to the flow in an expanding axisymmetric thin film shows that the curvature of the film is singular at a finite radius determined by a critical value of the Weber number. This singularity arises from the wall-normal momentum conservation which implies that $d^2h/dr^2 \rightarrow \infty$ whereas $(dh/dr)^2 \rightarrow 0$ at a finite radius. In § 3.1, we presented a physical mechanism to demonstrate the mechanical and surface energy exchange in steady flow. Physically, in the thin-film limit, $h'' = (1 + h'^2)(d\alpha/dr) \approx d\alpha/dr$, and the singularity implies that this change in interface slope $d\alpha/dr$ coincides with the hydraulic jump. Therefore, the mathematical expression in tandem with the physical interpretation indicates a jump. We also show that a similar jump condition can be obtained by applying conservation of radial momentum.

Using conservation of energy Bhagat *et al.* (2018) showed that the radial velocity gradient is also singular, in this case $dh/dr \rightarrow \infty$, at a critical Weber number which is numerically slightly different. This radius was identified in experiments as a jump in the flow depth to a thicker and slower flow downstream, and excellent quantitative agreement was found in the predicted and observed values of the jump radius.

There is a small numerical difference between the two predictions of the jump radius R given by conservation of energy and momentum, respectively, namely

$$\frac{R}{R_{ST}} = \left(\frac{1}{f'(0)(2\pi)^3} \frac{C_2}{C_1^3} \right)^{1/4} = 0.2705 \quad \text{and} \quad \left(\frac{1}{f'(0)(2\pi)^3} \frac{C_3}{C_1^3} \right)^{1/4} = 0.2481.$$

These numerical values are obtained from Watson's similarity profile which, as acknowledged, is only an approximation to the flow in the film, and the predictions are both smaller than the experimentally measured values of 0.289 ± 0.015 . Since C_1 is the area under the curve $f(\eta)$ then this will be smaller for the real profile (figure 3), leading to a larger prediction. Also, since $0 \leq \eta \leq 1$, $C_2 > C_3$, the jump radius estimate from momentum conservation is always smaller than that obtained from energy conservation, suggesting that energy is dissipated in the jump.

Acknowledgements

R.K.B. wishes to thank his PhD supervisor Professor D. I. Wilson for his advice and support.

Declaration of interests

The authors report no conflict of interest.

Appendix A. Scaling relation including gravity and surface tension

Bhagat *et al.* (2018) provided a scaling relationship for the jump radius R_{ST} from the following three conditions: (i) that the radial flow velocity u and depth h is balanced by viscous drag, $u/R \sim \nu/h^2$, (ii) continuity $uRh \sim Q$ and (iii) the jump is surface tension dominated, which implies at the jump, the Weber number $We = \rho u^2 h / \gamma \approx 1$. Further, their theoretical analysis including gravity gave the condition of hydraulic jump to be

$$\frac{1}{We} + \frac{1}{Fr^2} = 1, \quad (\text{A } 1)$$

where the Froude number $Fr = u/\sqrt{gh}$. Incorporating both gravity and surface tension through the use of (A 1) modifies the scaling relation (2.1) in the form

$$R \sim R_{ST} \left[\sqrt{\left(\frac{Q_C}{Q}\right)^2 + 2\left(\frac{Q_C}{Q}\right)} - \left(\frac{Q_C}{Q}\right) \right]^{1/4}. \quad (\text{A } 2)$$

As discussed in § 2, this gravitational correction to the radius R_{ST} determined by surface tension alone is 5% for $Q = 2Q_C$ and 23% for $Q = 10Q_C$.

Appendix B. Self-similar velocity profile

Following Watson's (1964) analysis, the conventional literature on the hydraulic jump (e.g. Bohr *et al.* 1993; Bush & Aristoff 2003; Kasimov 2008) assumes a self-similar velocity profile of the form

$$u(r, z) = u_s(r)f(\eta), \quad \eta \equiv \frac{z}{h(r)}, \quad 0 \leq \eta \leq 1,$$

where u_s is the surface velocity and $f(0) = 0, f(1) = 1, f'(1) = 0$. which further implies (see Watson 1964) that

$$\mathbf{u} = u_s(r)f(\eta)\hat{r} + u_s(r)h'(r)\eta f(\eta)\hat{z}. \quad (\text{B } 1)$$

Here, we will show that the conventional self-similar velocity profiles do not satisfy the zero interfacial shear-stress condition or $(\mathbf{n} \cdot \nabla)\mathbf{u} \neq 0$. We write

$$(\mathbf{n} \cdot \nabla)\mathbf{u} = \left(-\sin \alpha \frac{\partial}{\partial r} + \cos \alpha \frac{\partial}{\partial z} \right) (u_s(r)f(\eta)\hat{r} + u_s(r)h'(r)\eta f(\eta)\hat{z}) \quad (\text{B } 2)$$

or

$$\begin{aligned} & \left[-\sin \alpha \frac{du_s}{dr} f(\eta) - \sin \alpha u_s \frac{h'}{h} \eta f'(\eta) + \frac{1}{h} \cos \alpha u_s f'(\eta) \right] \hat{r} \\ & + \left[-\sin \alpha h' \frac{du_s}{dr} \eta f(\eta) - \sin \alpha h'' u_s \eta f(\eta) + \sin \alpha h' u_s \eta f'(\eta) \frac{h'}{h} \right. \\ & \left. + \sin \alpha h' u_s \frac{h'}{h} \eta^2 f'(\eta) + \cos \alpha u_s \frac{h'}{h} f(\eta) + \cos \alpha u_s \frac{h'}{h} \eta f'(\eta) \right] \hat{z}. \end{aligned} \quad (\text{B } 3)$$

Evaluating $(\mathbf{n} \cdot \nabla)\mathbf{u}$, equation (B 3) at the free surface with boundary conditions, $f(1) = 1$ and $f'(1) = 0$ yields

$$\left[-\sin \alpha \frac{du_s}{dr} \right] \hat{r} + \left(-\sin \alpha h' \frac{du_s}{dr} - \sin \alpha h'' u_s + \sin \alpha h' u_s \frac{h'}{h} + \cos \alpha u_s \frac{h'}{h} \right) \hat{z} \quad (\text{B } 4)$$

or

$$\begin{aligned} & -\frac{h'}{(1+h^2)^{1/2}} \frac{du_s}{dr} \hat{r} + \left(-\frac{h^2}{(1+h^2)^{1/2}} \frac{du_s}{dr} - \frac{h'h''u_s}{(1+h^2)^{1/2}} + \frac{1}{h} \frac{h^3u_s}{(1+h^2)^{1/2}} \right. \\ & \left. + \frac{1}{h} \frac{h'}{(1+h^2)^{1/2}} u_s \right) \hat{z}. \end{aligned} \quad (\text{B } 5)$$

The analysis implies that only for a completely flat film for which $h' = 0$ and $\mathbf{n} = \hat{z}$, $(\mathbf{n} \cdot \nabla)\mathbf{u} = 0$ can be trivially satisfied. In all other cases the tangential stress is non-zero.

REFERENCES

BATCHELOR, G. K. 2000 *An Introduction to Fluid Dynamics*. Cambridge University Press.
 BHAGAT, R. K., JHA, N. K., LINDEN, P. F. & WILSON, D. I. 2018 On the origin of the circular hydraulic jump in a thin liquid film. *J. Fluid Mech.* **851**, R5.
 BOHR, T., DIMON, P. & PUTKARADZE, V. 1993 Shallow-water approach to the circular hydraulic jump. *J. Fluid Mech.* **254**, 635–648.
 BUSH, J. W. M. & ARISTOFF, J. M. 2003 The influence of surface tension on the circular hydraulic jump. *J. Fluid Mech.* **489**, 229–238.
 BUTTON, E. C., DAVIDSON, J. F., JAMESON, G. J. & SADER, J. E. 2010 Water bells formed on the underside of a horizontal plate. Part 2. Theory. *J. Fluid Mech.* **649**, 45–68.
 DUCHESNE, A., ANDERSEN, A. & BOHR, T. 2019 Surface tension and the origin of the circular hydraulic jump in a thin liquid film. *Phys. Rev. Fluids* **4** (8), 084001.
 DUCHESNE, A., LEBON, L. & LIMAT, L. 2014 Constant Froude number in a circular hydraulic jump and its implication on the jump radius selection. *Europhys. Lett.* **107** (5), 54002.
 FERNANDEZ-FERIA, R., SANMIGUEL-ROJAS, E. & BENILOV, E. S. 2019 On the origin and structure of a stationary circular hydraulic jump. *Phys. Fluids* **31** (7), 072104.
 KASIMOV, A. R. 2008 A stationary circular hydraulic jump, the limits of its existence and its gasdynamic analogue. *J. Fluid Mech.* **601**, 189–198.

- MOHAJER, B. & LI, R. 2015 Circular hydraulic jump on finite surfaces with capillary limit. *Phys. Fluids* **27** (11), 117102.
- ROJAS, N. O., ARGENTINA, M., CERDA, E. & TIRAPEGUI, E. 2010 Inertial lubrication theory. *Phys. Rev. Lett.* **104** (18), 187801.
- SCHEICHL, B. 2019 Centred splash of a vertical jet on a horizontal rotating disc: recent findings and resolving controversies over the hydraulic jump. Available at: <https://pdfs.semanticscholar.org/ac9c/f5572c8fbc82e44ac87bb8bb4bc13a6a6016.pdf>.
- SEN, U., CHATTERJEE, S., CROCKETT, J., GANGULY, R., YU, L. & MEGARIDIS, C. M. 2019 Orthogonal liquid-jet impingement on wettability-patterned impermeable substrates. *Phys. Rev. Fluids* **4**, 014002.
- WANG, Y. & KHAYAT, R. E. 2019 The role of gravity in the prediction of the circular hydraulic jump radius for high-viscosity liquids. *J. Fluid Mech.* **862**, 128–161.
- WATSON, E. J. 1964 The radial spread of a liquid jet over a horizontal plane. *J. Fluid Mech.* **20** (3), 481–499.